

AD 639 754

TECHNICAL INFORMATION SERIES

MHD GENERATOR AND ACCELERATOR  
EXPERIMENTS IN SEEDED AND UNSEEDED  
AIR FLOWS

Best Available Copy

D D C

OCT 10 1966

C. J. HARRIS  
C. H. MARSTON  
W. R. WARREN, JR.

SPACE SCIENCES  
LABORATORY

CLEARINGHOUSE FOR FEDERAL SCIENTIFIC AND TECHNICAL INFORMATION		
50	29	75
MICROFICHE		

GENERAL  ELECTRIC

20040702058

# SPACE SCIENCES LABORATORY

EXPERIMENTAL FLUID PHYSICS SECTION

MHD GENERATOR AND ACCELERATOR EXPERIMENTS  
IN SEEDED AND UNSEEDED AIR FLOWS

By

Clarence J. Harris  
Charles H. Marston  
Walter R. Warren, Jr.

This work was supported by the United States Air Force,  
Contracts AF 04(647)-269 and AF 40(600)-1091; and presented  
at the International Symposium on MHD Electric Power Generation  
in Salzburg, Austria, July 4-8, 1966

September 1966  
R66SD50

MISSILE AND SPACE DIVISION

GENERAL  ELECTRIC

427983074

500740000

# TABLE OF CONTENTS

	PAGE
SUMMARY	2
SEEDED AIR FLOW STUDY	2
UNSEEDED AIR STUDY	9
CONCLUSIONS	13
SYMBOLS	15
REFERENCES	17

## SUMMARY

Two types of MHD experiments have been conducted at our laboratory using air flows produced by hypersonic shock tunnels. One experimental program was designed to evaluate the feasibility of using the Lorenz forces developed in an MHD generator for the attitude control of a hypervelocity vehicle. During this study the electrical conductivity of the seeded shock layer flow about a blunt model located in the shock tunnel test section was investigated along with the effect of pre-heating the generator electrodes. In the second experimental program, a Faraday accelerator is being studied to determine its ability to add kinetic energy to a high density, unseeded air flow in a high enthalpy shock tunnel. Measurements were made of the gross electrical conductivity of the flow, with and without an applied magnetic field. The meaning of the electrical conductivity measurements for each of these experiments is discussed.

## SEEDED AIR FLOW STUDY

In this study (1) electrical power was extracted from an MHD channel imbedded in the seeded air shock layer flow field about a blunt model and observations were made both of electrode phenomena and gross electrical conductivity. The study was conducted with a sting supported blunt wedge model in a combustion driven shock tunnel (2) having a 76 cm test section diameter. An air core electromagnet which produced a 1.4 Tesla pulsed

field mutually perpendicular to the model wall and the direction of flow was rigidly mounted inside the model. The shock tunnel was operated in the non-reflected configuration with a nominal shock Mach number,  $M_s = 11$ , and an initial driven tube pressure of 10 torr. The experimental MHD configuration is shown in Fig. 1a. The free stream test section flow was unseeded but the hypersonic shock layer generated about the model was seeded by introducing potassium salt from the model surface, just downstream of the stagnation line of the blunt model. A technique was provided (3) to prevent the seed material, potassium bicarbonate, from being trapped in the boundary layer and to assure its introduction into the inviscid shock layer. Spectroscopic measurements were made and showed that shock layer seeding had occurred (3). Separate measurements were made of the generator performance with room temperature and pre-heated electrodes. The resulting generator load lines were used to estimate gross electrical conductivity and electric power output. (See Fig. 6)

Further details of the experimental set-up and some of the results obtained in this study have been reported in References 3 and 4. The performance of the MHD generator was interpreted in References 3 and 4 on the assumption that the shock tunnel properties and model shock layer properties could be calculated assuming equilibrium flow. The equilibrium assumption will be re-evaluated here in the light of recent theoretical and experimental work in the area of defining non-equilibrium shock tunnel test section and model shock layer flow properties of air.

The MHD generator and electrical conductivity results of the previous experiment are re-evaluated accordingly.

High enthalpy expanding air non-equilibrium properties have been presented in graphical form in References 5 and 6. These results show the dependence of the final chemical composition upon the stagnation or plenum entropy value. The effective plenum conditions for both non-reflected and reflected shock tunnel operation are shown in Fig. 2. From the diagram in Fig. 2 it is observed that the effective stagnation enthalpy ( $H/RT_0$ ) for this study was 160 at an entropy value ( $S/R$ ) of 36.6. The frozen chemistry for these reservoir stagnation conditions are presented in the air Mollier diagram of Fig. 3. The Mollier diagram shows this test point regime and various non-equilibrium boundaries (6) (22) (23). These boundaries are discussed in detail in Reference 6. Below the "% O<sub>2</sub> Content" line in Fig. 3, the chemistry is frozen and this frozen chemistry is defined simply by the plenum entropy value ( $S/R$ ). This correlation with entropy, as presented in References 5 and 6 is based primarily upon non-equilibrium nozzle flow calculations made for an area ratio ( $A/A^*$ ) expansion of  $10^3$ , at an  $\ell$  value of 1 cm --- where  $\ell$  is defined from the physical geometry of the nozzle based upon the relationship  $A/A^* = 1.0 + (\frac{x}{\ell})^2$ , (7). The term  $x$  is the axial distance along the nozzle measured from the nozzle throat. In the MHD study the flow was expanded through an area ratio of 25 and the equivalent  $\ell$  value was 28 cm. Allowing for this larger  $\ell$  value, the expansion

still yields enthalpy values below the "% O<sub>2</sub> Content" line and therefore test section conditions in the non-equilibrium frozen flow regime. In view of these results the equilibrium assumption in the earlier reports (1) (3) is no longer valid.

The correlation approach of References 5 and 6 used to define the test section chemical composition as a function of plenum entropy has also been applied in defining the electron concentration (hence electrical conductivity) for an expanding air flow. The resulting electron concentration - entropy dependence is shown in Fig. 4 based on the results of References 8 and 9. The  $l = 10$  cm results, of course, more closely approximate the conditions existing in the MHD study. At an entropy ratio value,  $S/R = 36.6$ , the electron concentration value is expected to be of the order of  $1 \times 10^{-9}$  moles/gm of mixture. Kaegi and Chin (10) have shown that the experimentally measured electron concentration in expanded non-equilibrium test section flows is an order of magnitude or more greater than the analytically predicted concentration obtained from the correlation of Fig. 4. Using both the experimental results of Reference 10 and the analytically derived electron-concentration correlation (Fig. 4) as guides, the test section electron concentration for the MHD experiment is estimated to be of the order of  $10^{-8}$  moles/gm of mixture in a non-equilibrium chemically frozen flow. The higher experimental electron concentration value is assumed to be due to the fact that the electron temperature is frozen at a temperature higher than

that of the chemical species in the non-equilibrium frozen flow (10) (11).

Next it is necessary to determine the flow properties in the shock layer. The experimental measurements of Reference 10 again offer a guide in predicting the expected electron concentration in the stagnation point region of a blunt body under free stream flow conditions approximating those in the MHD study. The predicted equilibrium stagnation point conditions (13) yield a stagnation pressure of 1.2 atmospheres and a stagnation temperature of 5300°K. The stagnation point Reynolds number,  $Re_s = \frac{\rho_{\infty} v_{\infty} R_{\infty}}{\mu_s}$ , exceeds 2000 and therefore the higher density results of Reference 10 are more applicable in evaluating the MHD experiment. The electron concentration at the model stagnation point therefore is defined by the inviscid stream tube analysis (10) (12). This analysis when applied here as in Reference 10 gives an electron concentration value at the stagnation point stream tube within a factor of 3 of the equilibrium value of  $10^{14}$  electrons/cc (3). Thus, at the model stagnation point the electron concentration is reasonably close to the equilibrium value even though the free stream chemical (5) (6) and thermodynamic (22) properties are frozen at the non-equilibrium value and the free stream electron temperature is elevated above that of the non-equilibrium flow.

The electron concentrations in the portions of the expanding shock layer flow field downstream of the stagnation point may be estimated using the approximate non-equilibrium analysis of Reference 14. The

non-equilibrium expansion from the stagnation point presented in Reference 14 is for the case where the gas temperature and electron temperature are the same (thermodynamic equilibrium). The results of Reference 10 lead one to postulate that the "two temperature" situation which existed for the nozzle flow expansion will also occur to some extent for the shock layer flow expansion. This would result in the shock layer electron concentration values downstream of the stagnation point being larger than the non-equilibrium "one temperature" predicted value. Eschenroeder (15) has shown that the downstream shock layer electron concentration values for an equilibrium expanded flow and a non-equilibrium "one temperature" expanded flow approach the same value. Therefore, assuming a "two temperature" non-equilibrium shock layer expansion from the equilibrium stagnation point conditions, the electron concentration may be expected to be approx. an order of magnitude greater in value than that predicted for an equilibrium shock layer expansion. The unseeded air equilibrium electrical conductivity value,  $\sigma$  at the entrance to the MHD generator is quite low, of the order of  $10^{-3}$  mhos/meter and a one or two order of magnitude increase is insignificant for producing values leading to meaningful MHD effects. Therefore, in this experiment it is the introduction of a seed material into the shock layer flow that produces the required enhancement in electrical conductivity. The actual  $\sigma$  value at the MHD generator therefore depends upon the type of expansion (equilibrium, non-equilibrium "one temperature", non-equilibrium "two

temperature", frozen stagnation, etc.) that the seeded flow undergoes from the model stagnation point to the downstream model station. The experiments of Reference 16 give some indication of the phenomena to be expected in seeded flows. The  $\sigma$  values obtained by Zukoski, et al in Reference 16 were 50% smaller than the  $\sigma$  values predicted using the two temperature model offered by Kerrebrock (11). Zukoski, et al (12) also show experimentally that the time to achieve a steady state electron temperature in a constant temperature gas is quite short, of the order of  $50 \mu$  second. In the MHD experiment the flow time of a gas particle from the model stagnation region to the entrance of the MHD generator was estimated to be of the order of  $50 \mu$  second (13). The actual test time duration in this study is of the order of 1 millisecond as determined from the generator induced voltage-time characteristics (Fig. 5). The induced potential obtained with the loaded generator is observed to rise rapidly and be relatively constant for approximately 1 millisecond before dropping off abruptly. Assuming that a "one temperature" non-equilibrium expansion from the stagnation point takes place, the electrical conductivity of the flow, seeded with potassium bicarbonate, at the entrance to the MHD generator will be 25 mhos/meter (since the equilibrium and "one temperature" non-equilibrium values are approximately equal).

The MHD generator voltage-current characteristics from this study are presented in Fig. 6 for the cases where both electrodes were initially at room temperature and the case where the emitting electrode (made of

lanthanum hexaboride, La B<sub>6</sub>) was externally heated to 1300° C prior to the arrival of the test flow. As reported previously (1) (3) these generator load-lines yield different values of generator gross electrical conductivity. The interesting result is that the situation where the electrode was heated yields a generator gross (or bulk) electrical conductivity value very close to the value obtained analytically by assuming equilibrium expanding nozzle flow and an equilibrium or "one temperature" non-equilibrium seeded shock layer flow about the model. The measured  $\sigma$  value with a heated electrode is 20 mhos/m. The Hall parameter,  $\omega\tau$  for this study is  $\sim 1.0$  resulting in a scalar  $\sigma$  value of 40 mhos/m; in excess of the equilibrium or "one temperature" non-equilibrium prediction and therefore implying that "two temperature" non-equilibrium effects may be present. The increase by a factor of seven in generator gross electrical conductivity, apparently due to electrode pre-heating may be attributed to either electrode surface effects (work function), aerodynamic boundary layer effects (modification of boundary layer profiles due to the hot wall), or a combination of both. Similar effects will be discussed in the next section in conjunction with the electrode effects observed in an MHD accelerator experiment in which unseeded air was the test gas.

#### UNSEEDED AIR STUDY

In a study presently being conducted in our laboratory a Faraday accelerator has been designed, built, and operated (17) (18) in conjunction with an electrically driven, high density, reflected shock tunnel (19). The

accelerator is designed to operate at static pressures and temperatures of the order of 30 atmospheres and  $7000^{\circ}\text{K}$  respectively. The expanding air flow in this study is unseeded air and its average equilibrium scalar electrical conductivity is estimated to be of the order of 150 mhos/meter with a Hall parameter value,  $\omega\tau$  of the order of 1.0. The entrance velocity is approximately 4,300 m/sec. The accelerator is 31 cm in length, has 38 pairs of segmented electrodes - each separately powered, has a square cross-section (1.27 cm x 1.27 cm at the entrance and 1.78 cm x 1.78 cm at the exit) and operates using a 5.2 Tesla pulsed air-core magnet, Fig. 1b. A velocity increase of about 1500 m/sec is predicted, based on the one dimensional analysis of References 17 and 18.

One of the many factors affecting accelerator performance is the gross electrical conductivity of the ionized air and, therefore, the electrical currents capable of being drawn during testing. Further, electrode phenomena such as considered in the preceding section are again quite important. This portion of the paper will deal only with these gross electrical conductivity and electrode aspects of the study.

The conditions of this experiment were chosen so that the test gas electrical conductivity would be large enough to allow for the evaluation of the performance of the accelerator without the necessity of introducing a seed material. The state of the expanding air was determined analytically, again using the non-equilibrium correlation approach offered in Reference 6. The flow expands isentropically ( $S/R = 37.6$ )

from a reservoir enthalpy ( $H/RT$ ) value of 298 (Fig. 2) to a static enthalpy value of 194 at the entrance to the MHD accelerator. On the basis of the earlier discussion regarding the "percent oxygen content limit" shown in Fig. 3, the unseeded air will remain in equilibrium. We assume that this is the case and give no further consideration to non-equilibrium effects.

Experimental measurements have been made of the voltage gradients normal to the channel flow and the total electrode currents drawn at various stations along the channel--both with and without the applied magnetic field. Typical voltage gradient and current data are shown in Fig. 7 along with traces showing reservoir pressure and  $v \times B$  potential. The measurements obtained without an applied magnetic field were made by applying external electrical potentials to various pairs of electrodes--each pair taken as a separate circuit. The applied potential in these cases approximated the voltage gradient ( $E - vB$ ) expected across the channel for the case when the MHD interaction was present. In this study the electrodes were always initially at room temperature. The electrodes showed no physical evidence of damage due to electrical arcing, electron stripping, or electron bombardment.

The measurements obtained with the 5.2 Tesla pulsed magnetic field present were made in the normal MHD accelerator mode while applying external electrical potentials, again to each electrode pair as a separate circuit. In these tests it was observed that the electrodes

showed physical damage. There is apparently a distinct difference in the type of current conduction mechanism taking place at the anodes compared to that taking place at the cathodes. The cathodes, Fig. 8, show evidence only of material being lifted, or "etched" away, while on the anode (Fig. 8) there are indications of severe local heating resulting in the resolidification of molten copper on the electrode surface.

Results of measurements obtained at electrode station #6, which is located 3 cm from the channel entrance, are shown in Fig. 9; similar data were obtained at two other stations along the channel. In all cases two adjacent electrodes, upstream and two downstream of the measurement station were also electrically powered. Because the gas cools during isentropic expansion, but has approximately constant temperature during acceleration, the state of the gas for these two test conditions is quite different at the downstream stations; however, there is nominally no difference in the states of gas at the upstream stations. Therefore at station #6 which is close to the entrance, the gas properties should be approximately equal; with and without a B field.

The data of Fig. 9 have been used to infer the types of current limiting mechanisms in the accelerator. It is observed that the electrode current increases with increasing electrode voltage in such a manner that a reduction in the apparent electrical resistance is obtained. A lower voltage limit (100 volts) is defined from the data below which current conduction all but ceases. As the voltage is increased the gross electrode

current increases as expected but the apparent resistance decreases. With increasing voltage (over the range of values investigated) the bulk electrical conductivity may be interpreted as approaching the inviscid equilibrium value. Therefore, it appears that current conduction is limited by a mechanism at the electrode surface (such as the electrode sheath discussed by Zauderer (20) and Myers (24) ), and also by effects in the cool aerodynamic boundary layer. The electrode surface effect provides a constant loss mechanism defined quantitatively by the minimum voltage limit. Sherman (21) has also suggested that blowing of the current filaments by the high velocity test gas may be producing some of the effects observed here. The decrease in apparent resistance with increasing current is interpreted here to be a result of the Joule heating of the cool boundary layer.

### CONCLUSIONS

Non-equilibrium effects, when accounted for in the shock layer MHD generator experiment have negligible influence upon the original interpretation of the results. This is due primarily to the fact that seeding the shock layer flow is a first order effect which dominates the non-equilibrium effects of the unseeded air system at the flow conditions of this experiment. Pre-heating the electrodes greatly enhanced the performance of the MHD generator. This may be due to reduction in the electrode emitter work function, heating of the aerodynamic boundary layer, or a combination of both.

The loss mechanisms which reduce the magnitude of the gross electrical currents (and therefore the effective Lorentz force in the plasma) in the MHD accelerator have been tentatively classified as a combination of an electrode voltage drop independent of current level and a current dependent boundary layer loss. Experimentation is continuing in order to gain a more detailed insight into the manner in which these losses can be reduced.

## SYMBOLS

$A/A^*$	area ratio
$B$	magnetic field
$E$	electric potential gradient
$H$	enthalpy
$l$	nozzle scale parameter
$M_s$	shock Mach number
$O_2$	molecular oxygen
$P_1$	shock tube driven section initial pressure
$P_5, P_r$	reservoir pressure
$R$	gas constant
$r$	ohmic resistance
$R_b$	model nose radius
$Re_s$	stagnation point Reynolds number
$S$	entropy
$T_0$	temperature @ S. T. P.
$T_5$	reservoir temperature
$v$	particle velocity
$v_\infty$	free stream velocity
$x$	nozzle axial distance
$Z$	equilibrium oxygen dissociation
$\mu_s$	viscosity

SYMBOLS (Continued)

$\rho_{\infty}$  free stream density  
 $\sigma$  electrical conductivity

## REFERENCES

1. Harris, C. J. , "Initial Experimental Results of a MHD Flight Control Study", G. E. MSD Adv. Aero. Tech. Memo 116, Jan. 1961.
2. Warren, W. R. , Kaegi, E. M. , Harris, C. J. and Geiger, R. E. , "Shock Tunnel Studies of the Aerodynamics of Atmosphere Entry", G. E. R61-056, ARS.
3. Muntz, E. P. , Kaegi, E. M. and Harris, C. J. , "Techniques for Exper. Invest. of the Properties of Electrically Conducting Flow Fields", presented at the Second National Symposium on Hypervelocity Techniques, Denver, Colo. , March 1962.
4. Harris, C. J. and Johnson, R. H. , "An Experimental Evaluation of Several Attitude Control Concepts", presented at the Seventh Symposium on Ballistic Missile and Space Technology, Aug. 1962.
5. Harris, C. J. , "Comment on Nonequilibrium Effects on High Enthalpy Expansion of Air", AIAA Journal, June 1966, Vol. 4, No. 6.
6. Harris, C. J. and Warren, W. R. , Jr. , "Correlation of Nonequilibrium Chemical Properties of Expanding Air Flows", G. E. R64SD92, Dec. 1964.
7. Eschenroeder, A. Q. , "Exact Solutions for Nonequilibrium Expansions of Air with Coupled Chemical Reactions", C. A. L. Report No. AF-1413-A-1, May 1961.
8. Boyer, D. W. , "Nonequilibrium Nozzle Expansion Calculations for SSL, G. E. ", private communication.
9. Eschenroeder, A. Q. and Daiber, J. W. , "Ionization Nonequilibrium in Expanding Flows", ARS Paper 1458-60, Dec. 1960.
10. Kaegi, E. M. and Chin, R. , "Stagnation Region Shock Layer Ionization Measurements in Hypersonic Air Flows", AIAA Paper No. 66-167, March 1966.
11. Kerrebrock, J. L. , "Conduction in Gases with Elevated Electron Temp. , " Engineering Aspects of Magnetohydrodynamics, 1962.
12. McMenamin, D. L. , G. E. MSD, private communication.

13. Harris, C. J., "Some Aspects of a Shock Tunnel Study Involving the Application of MHD Forces to Vehicle Attitude Control", G. E. MSD Adv. Aero. Lab. TM #98, Feb. 1960.
14. Ellington, D. and Tremblay, R., "Nonequilibrium Electron Density Distributions in Hypersonic Air Flows Around Blunt Bodies", CARDE T.R. 503/64, July 1964.
15. Eschenroeder, A. Q., "Ionization Nonequilibrium in Expanding Flows", ARS Journal, Feb. 1962.
16. Zukoski, E. E., Cool, T. A. and Gibson, E. G., "Experiments Concerning Nonequilibrium Conductivity in a Seeded Plasma", AIAA Journ., Vol. 2, No. 8, 1964.
17. Feasibility Study of a High Density Shock Tunnel Augmented by a Magnetohydrodynamic Accelerator, AEDC-TR-65-225, Oct. 1965.
18. Harris, C. J., Marston, C. H., Warren, W. R., Mallin, J. and Rogers, D. A., "A High Density Shock Tunnel Augmented by a Faraday MHD Accelerator", presented at the Fourth Hypervelocity Techniques Symposium, Tullahoma, Tenn., Nov. 1965.
19. Warren, W. R., Harris, C. J., and Rogers, D. A., "The Dev. of an Electrically Heated Shock Driven Test Facility", Second Symp. on Hypervelocity Tech., Denver, March 1962.
20. Zauderer, B., "Electrical Characteristics of the Linear Hall and Faraday Generators at Small Hall Parameters", Seventh Symposium on Eng. Aspects of MHD, April 1966.
21. Sherman, A., G. E. SSL, private communication.
22. Lordi, J. A. and Mates, R. E., "Nonequilibrium Expansion of High Enthalpy Air Flows", Cornell Aeronautical Lab. Report AD-1716-A-3, March 1964.
23. Bray, K. N. C., "Atomic Recombination in a Hypersonic Wind Tunnel Nozzle", J. of Fluid Mechanics 6, (1959).
24. Myers, T. W., "Experimental Investigation of the Balancing Mechanism and Electrical Properties of an Argon Arc in Crossed Convective and Magnetic Fields", Seventh Symp. on Eng. Aspects of MHD, April 1966.

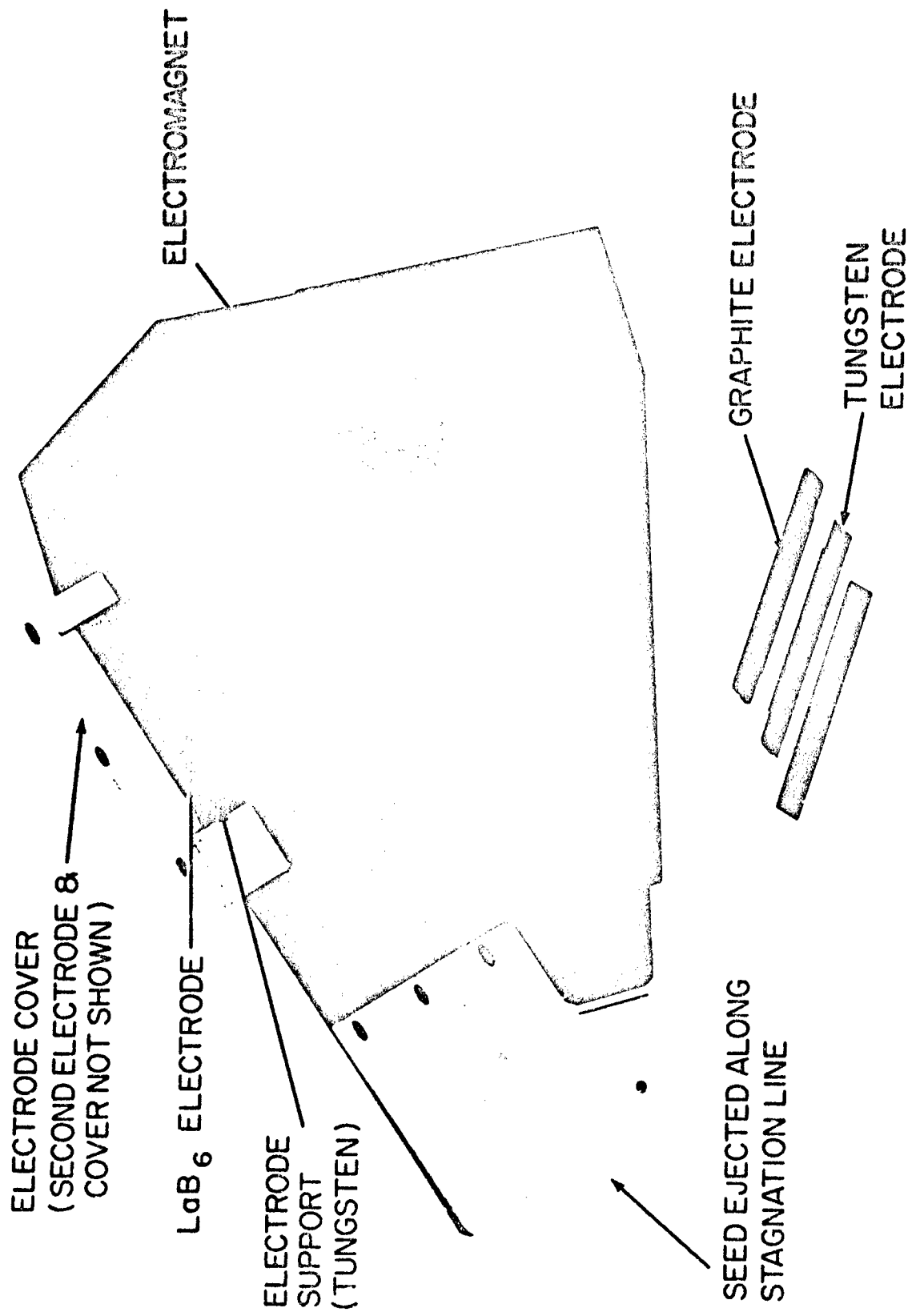


Figure 1a. MHD Generator Model

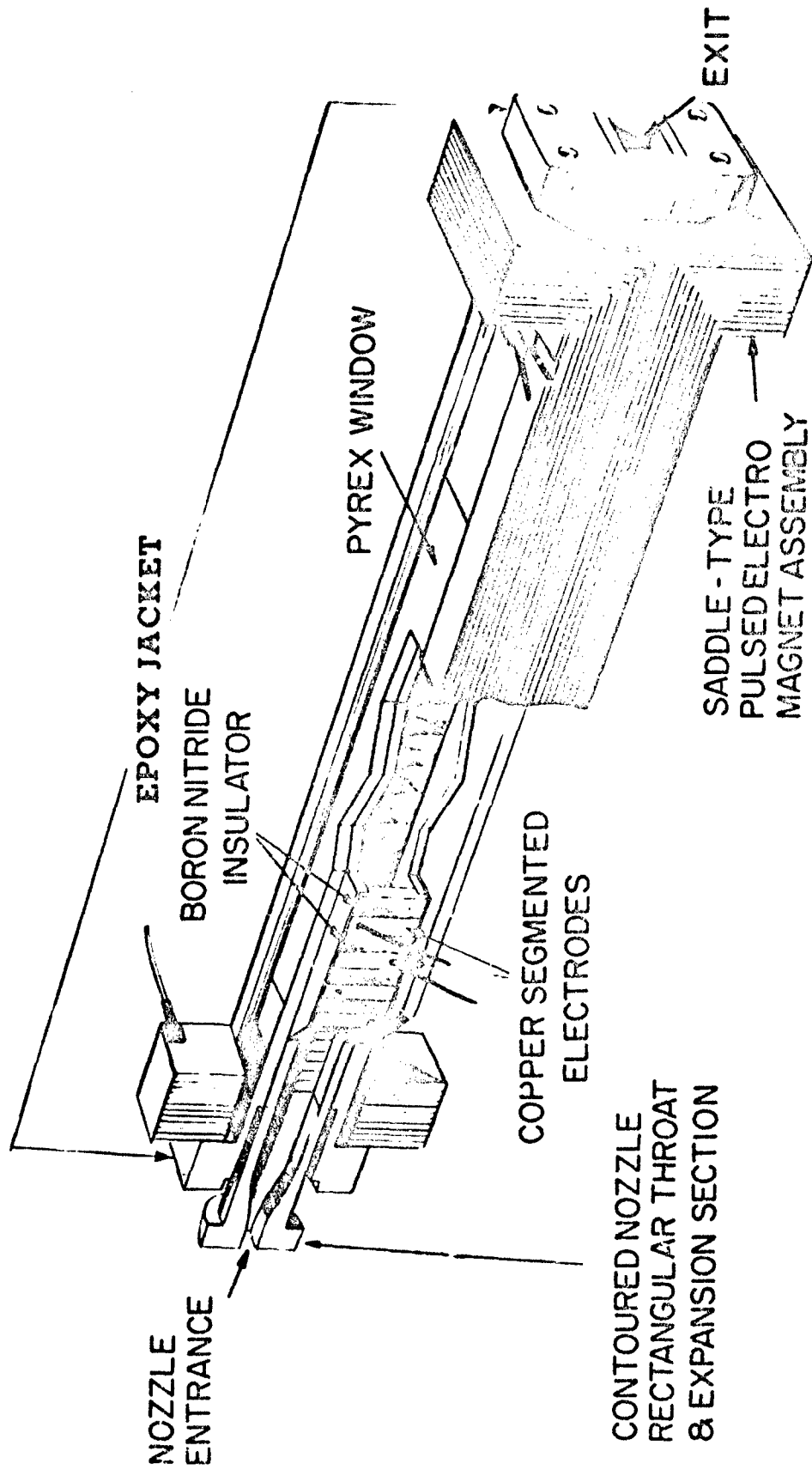
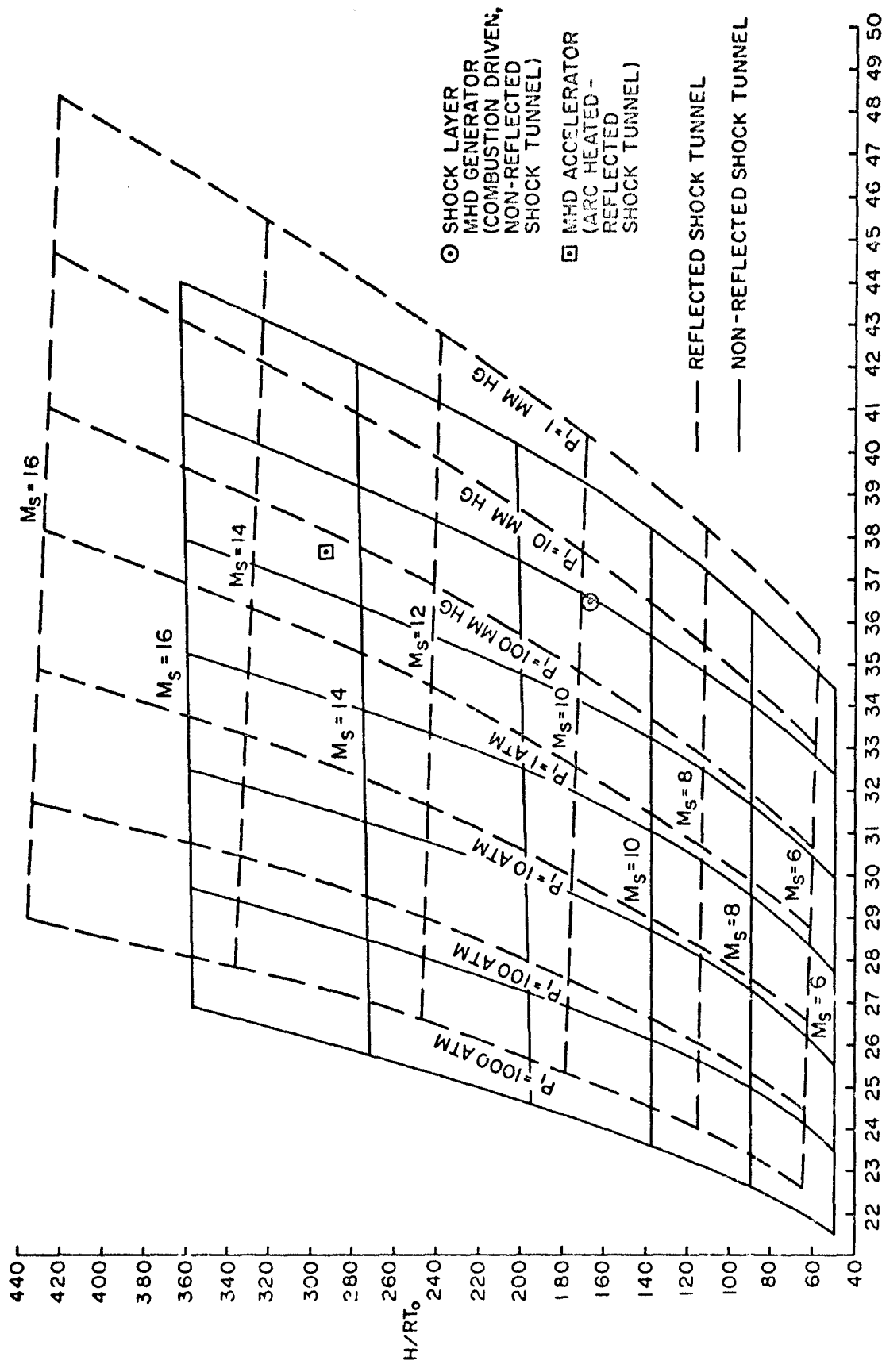


Figure 1b. MHD Accelerator



S/R

0103-177A

Figure 2. Effective Plenum Conditions for Reflected and Non Reflected Shock Tunnels Operating at Given Values of  $M_s$  and  $P$

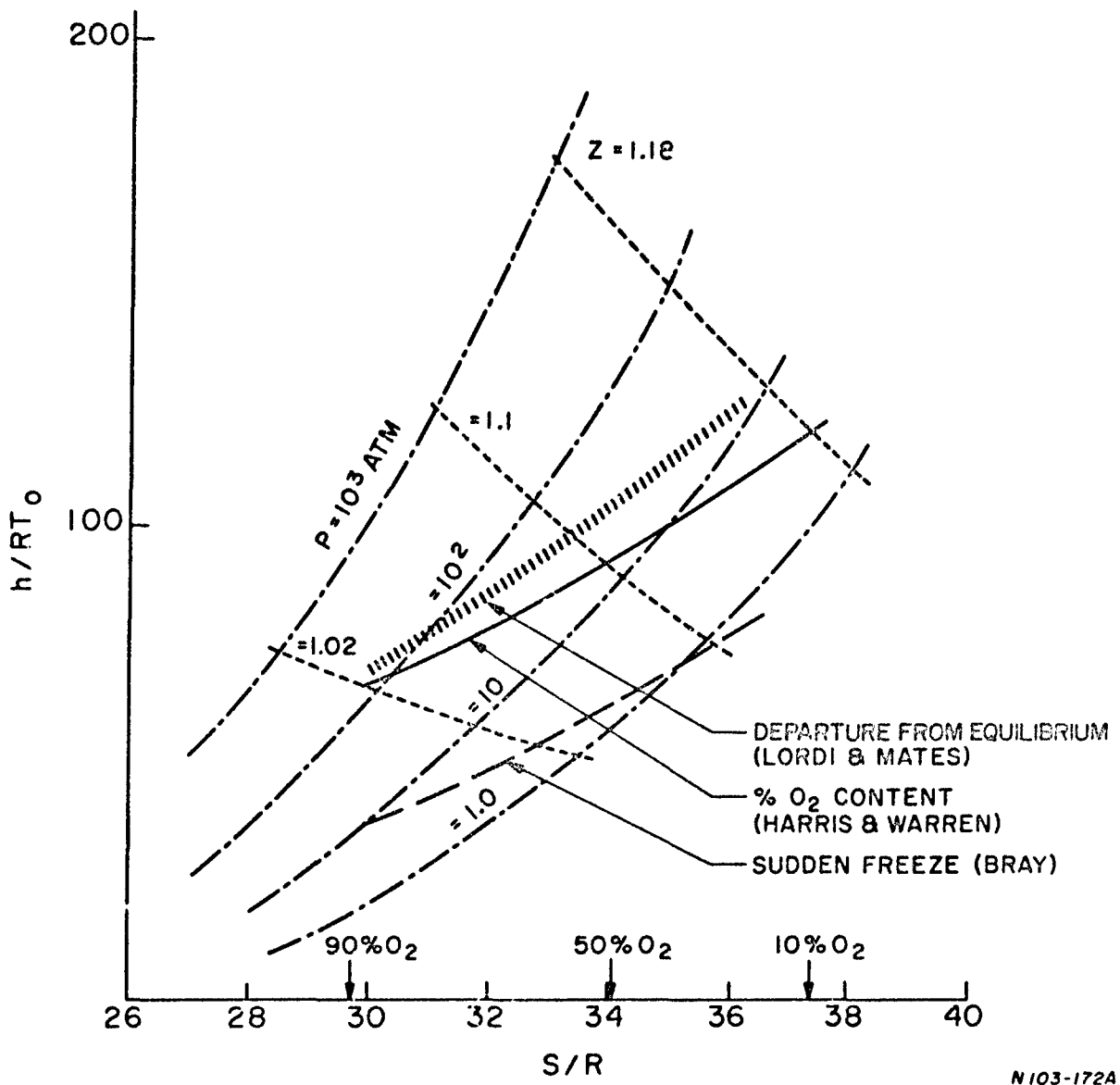


Figure 3. Air Mollier Diagram Showing Chemical Limit Lines Arising from Various Correlations of Non-equilibrium Expanding Flow Processes

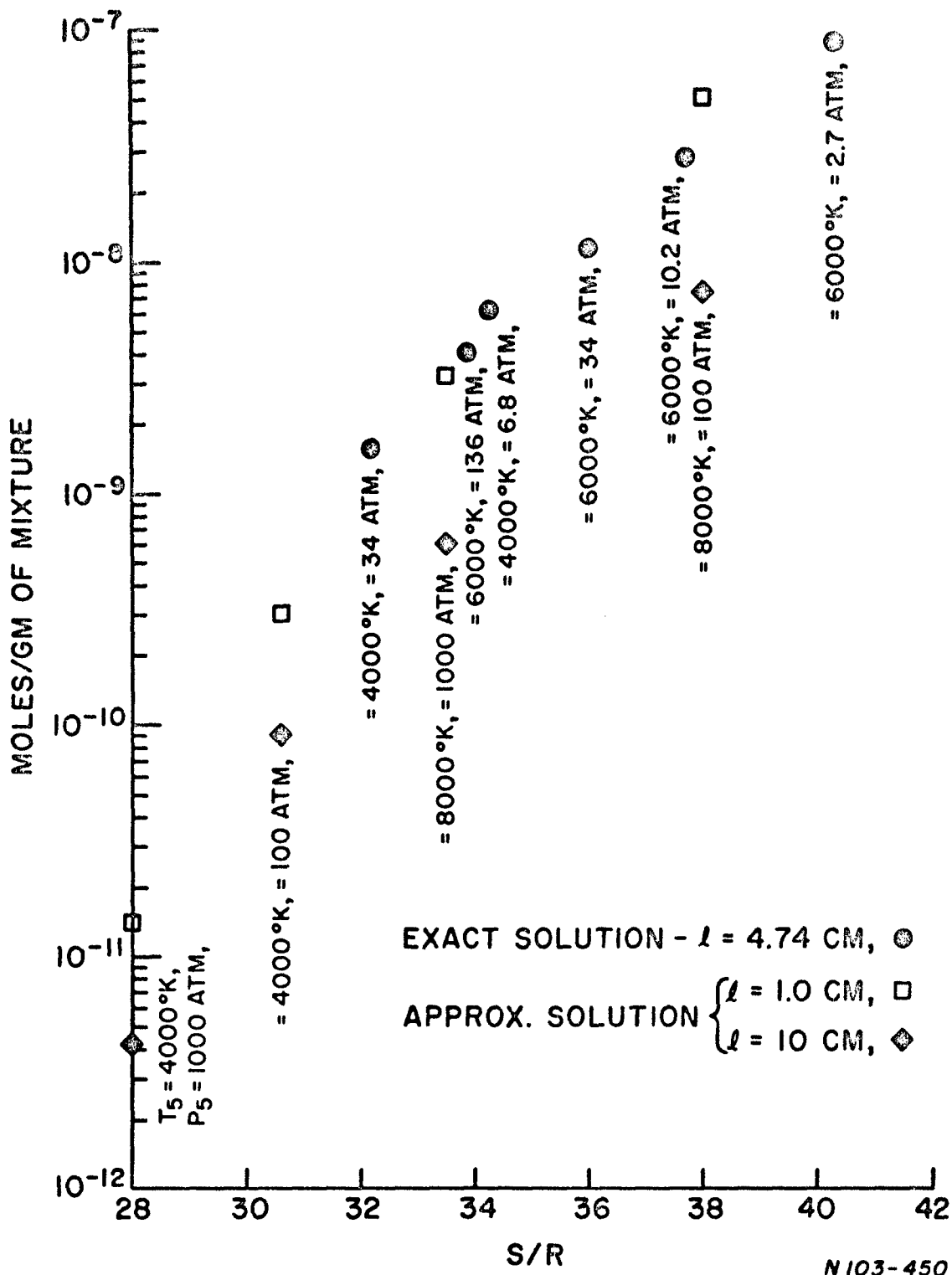
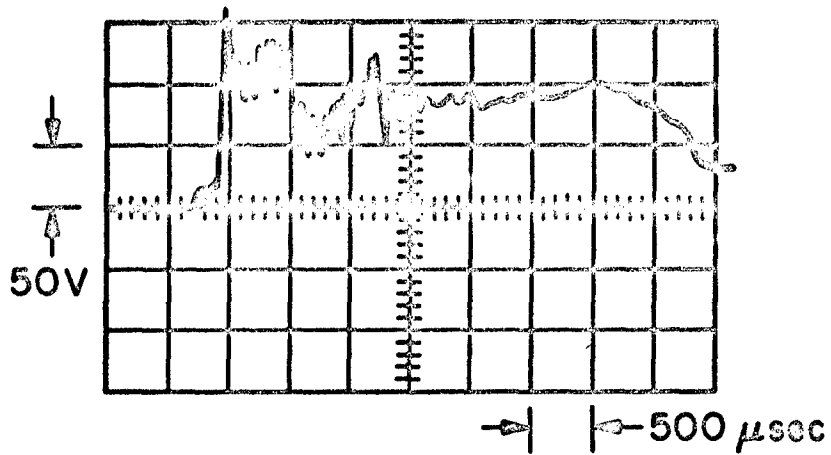
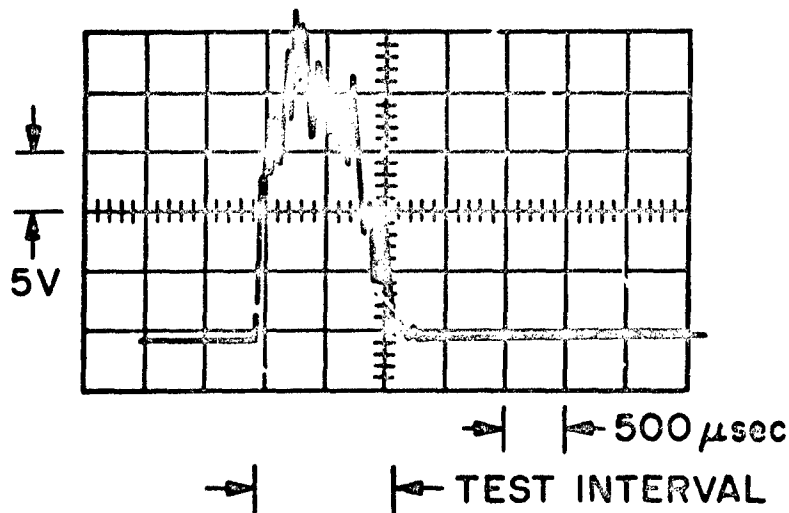


Figure 4. Non-equilibrium Electron Concentration Correlation with Reservoir Entropy @  $A/A_* = 10^3$



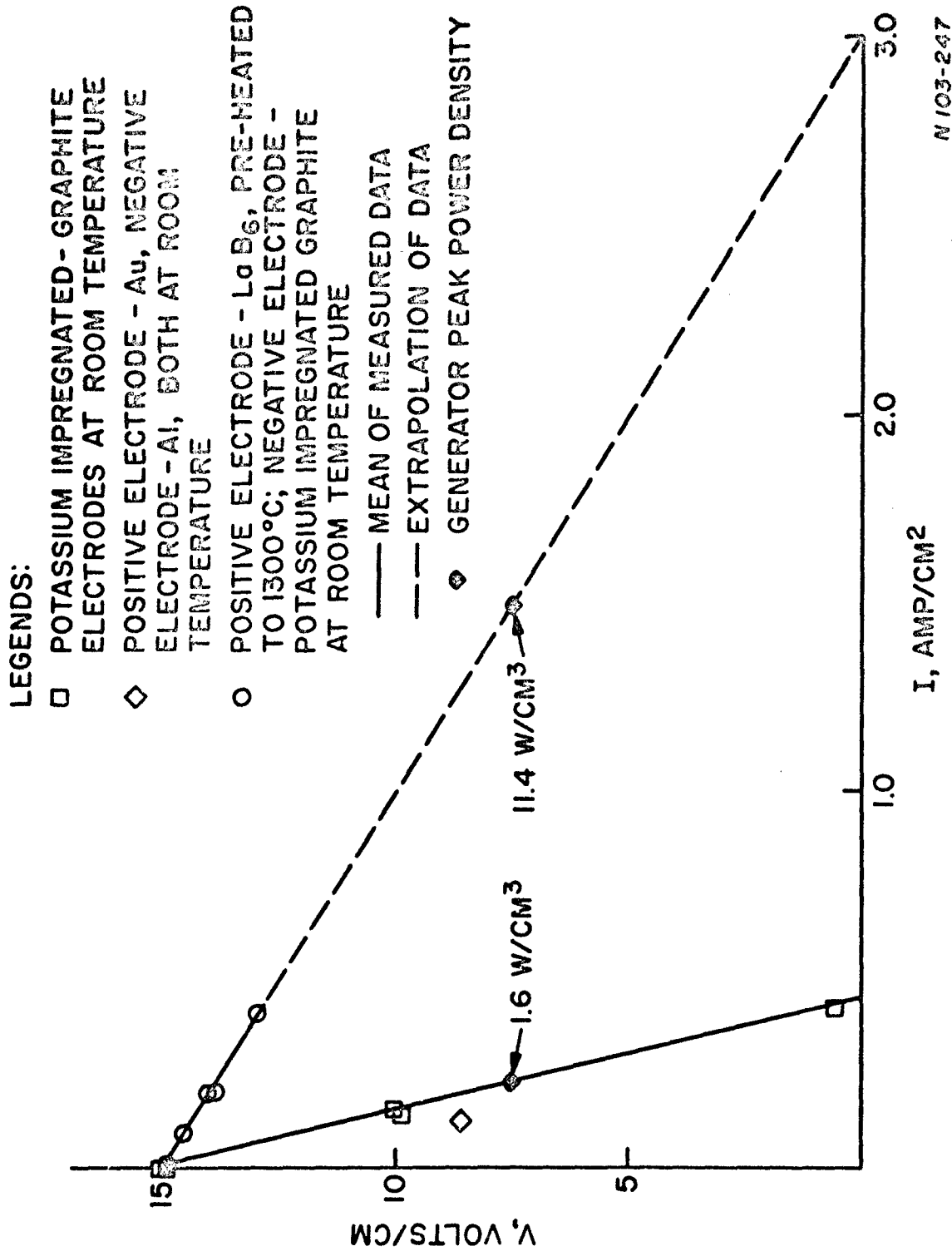
OPEN CIRCUIT INDUCED  $v \times B$  POTENTIAL



INDUCED  $v \times B$  POTENTIAL WITH A  $6.04 \Omega$  LOAD

N103-251

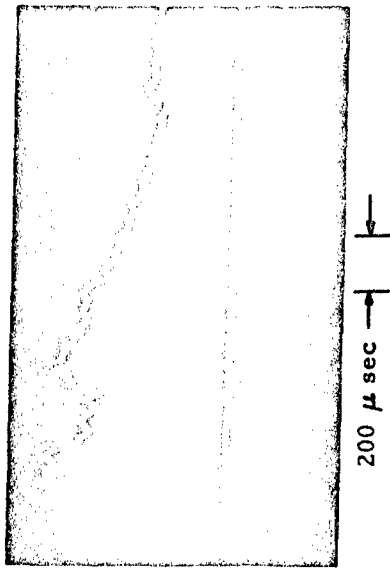
Figure 5. Induced EMF - Induced Electrical Current Characteristics in the MHD Generator



N 103-247

Figure 6. Load Characteristics of the MHD Generator

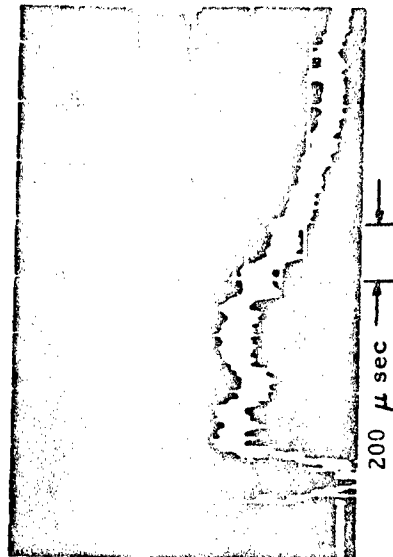
Reservoir Pressure



68 ATM

200 μsec

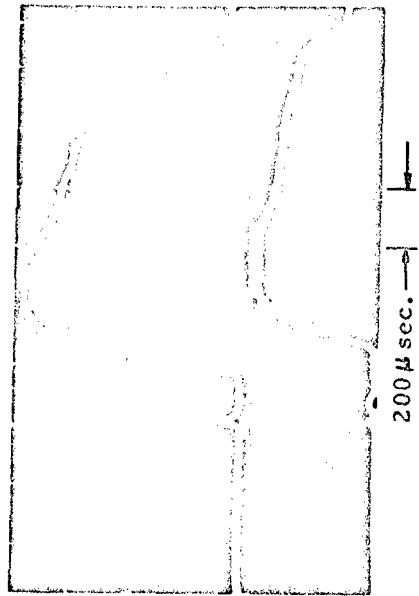
Electrode Current without B Field



40.7 Amp

200 μsec

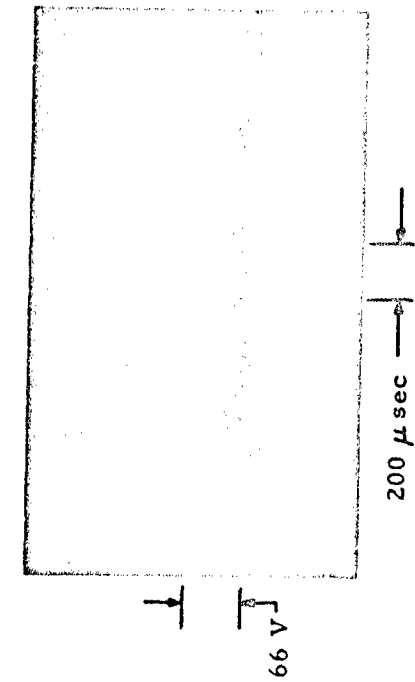
Electrode Current with B field



205 amp  
(Mid-Channel Sta.)

480 amp  
(Downstream Sta.)

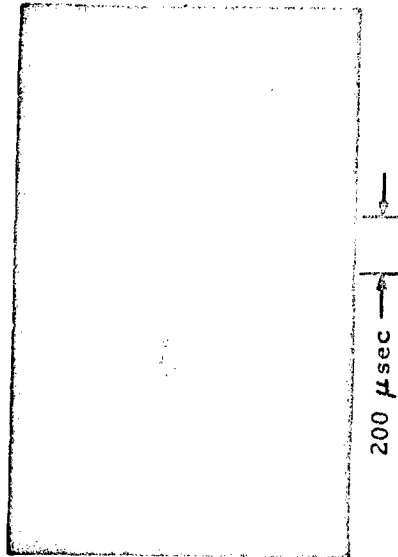
200 μsec



66 V

200 μsec

Voltage Gradient at Sta. #6 across central 60% of channel width, without B field

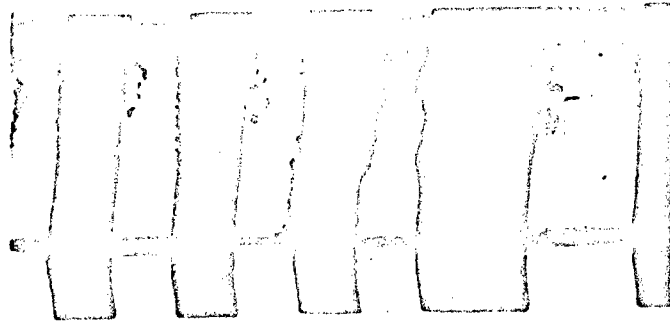


65V

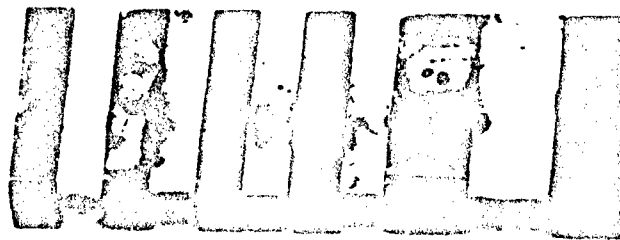
200 μsec

Open circuit,  $\mathcal{N} \times B$  potential at middle of channel,  $B_{ave} = 2.9$  Tesla

Figure 7. Characteristic Experimental Measurements in the MHD Accelerator



Cathodes - after one MHD Accelerator Test @  $B = 5.2$  Tesla



Anodes - after one MHD Accelerator Test @  $B = 5.2$  Tesla

Figure 8. Typical Surface Effects on the MHD Accelerator Cathodes and Anodes

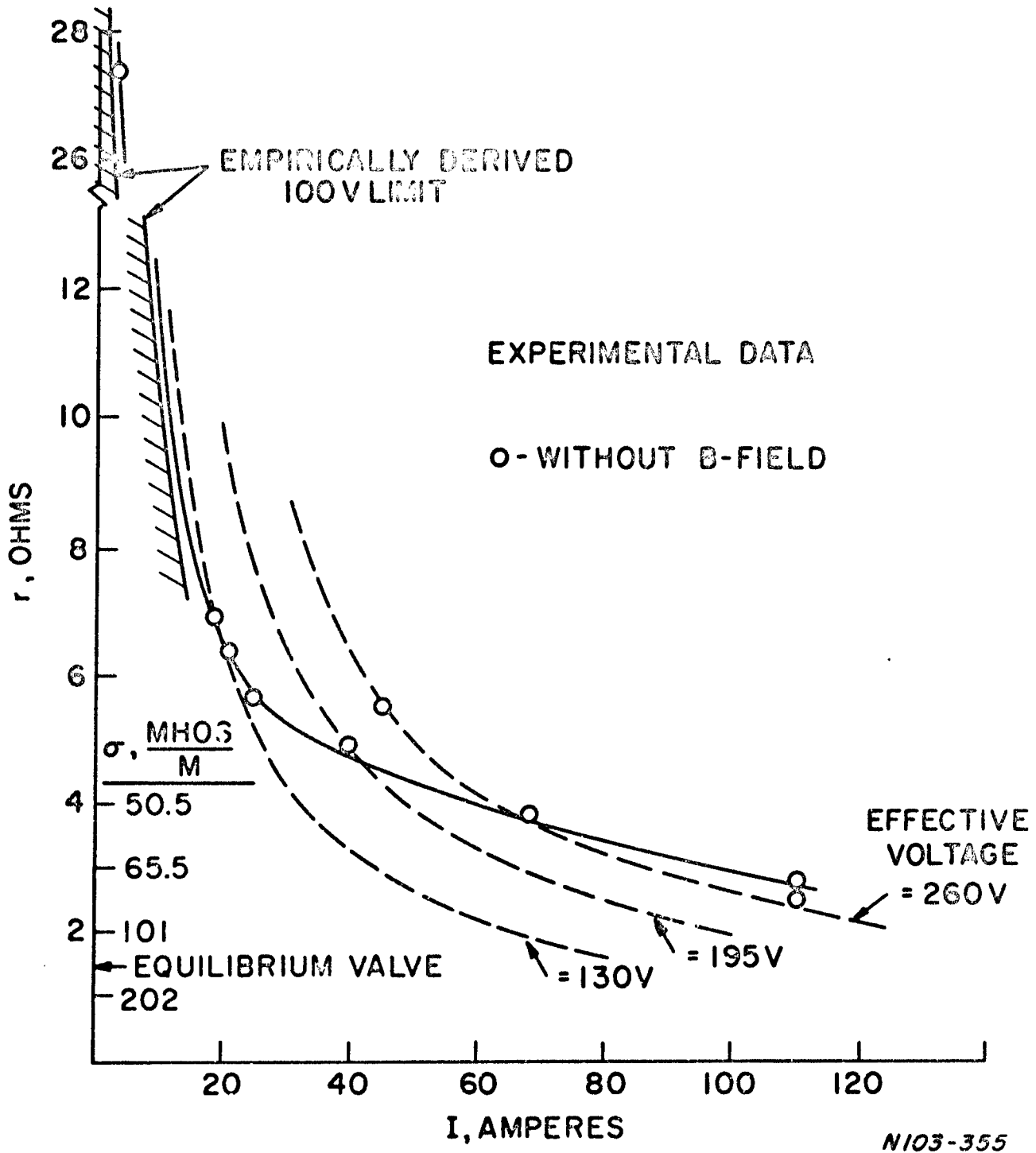


Figure 9. Relationship of MHD Accelerator Ohmic Resistance and Electrical Current

N103-355

SPACE SCIENCES LABORATORY  
MISSILE AND SPACE DIVISION

GENERAL ELECTRIC

TECHNICAL INFORMATION SERIES

AUTHOR C. J. Harris C. H. Marston W. R. Warren, Jr.	SUBJECT CLASSIFICATION MHD GENERATOR AND ACCELERATOR	NO. R66SD50
TITLE MHD Generator and Accelerator Experiments in Seeded and Unseeded Air Flows		DATE Sept. 1966
REPRODUCIBLE COPY FILED AT MOD LIBRARY, DOCUMENTS LIBRARY UNIT, VALLEY FORGE SPACE TECHNOLOGY CENTER, KING OF PRUSSIA, PA.		G. E. CLASS I GOV. CLASS Unclassified
SUMMARY <p>Two types of MHD experiments have been conducted at our laboratory using air flows produced by hypersonic shock tunnels. One experimental program was designed to evaluate the feasibility of using the Lorenz forces developed in an MHD generator for the attitude control of a hypervelocity vehicle. During this study the electrical conductivity of the seeded shock layer flow about a blunt model located in the shock tunnel test section was investigated along with the effect of pre-heating the generator electrodes. In the second experimental program, a Faraday accelerator is being studied to determine its ability to add kinetic energy to a high density, unseeded air flow in a high enthalpy shock tunnel. Measurements were made of the gross electrical conductivity of the flow, with and without an applied magnetic field. The meaning of the electrical conductivity measurements for each of these experiments is discussed.</p>		NO. PAGES 28
KEY WORDS Nonequilibrium effects, electrode effects		

BY CUTTING OUT THIS RECTANGLE AND FOLDING ON THE CENTER LINE, THE ABOVE INFORMATION CAN BE FITTED INTO A STANDARD CARD FILE

AUTHOR C. J. Harris C. H. Marston W. R. Warren, Jr.  
 COUNTERSIGNED W. R. Warren, Jr.